

# Constraining kaon PDFs from Drell-Yan and $J/\psi$ production

Wen-Chen Chang<sup>a,1</sup>, Jen-Chieh Peng<sup>b,c,2</sup>, Stephane Platchkov<sup>d,3</sup>, Takahiro Sawada<sup>e,4</sup>

<sup>a</sup>*Institute of Physics, Academia Sinica, Taipei 11529, Taiwan*

<sup>b</sup>*Department of Physics, University of Illinois at Urbana-Champaign, Urbana, IL 61801, USA*

<sup>c</sup>*Department of Physics, National Central University, Chung-Li, 32001, Taiwan*

<sup>d</sup>*IRFU, CEA, Université Paris-Saclay, 91191 Gif-sur-Yvette, France*

<sup>e</sup>*Institute for Cosmic Ray Research, The University of Tokyo, Gifu 506-1205, Japan*

---

## Abstract

The kaon parton distribution functions (PDFs) are poorly known due to paucity of kaon-induced Drell-Yan data. Nevertheless, these Drell-Yan data suggest a softer valence  $u$  quark distribution of the kaon compared to that of the pion. We discuss the opportunity to constrain the kaon PDFs utilizing the existing kaon-induced  $J/\psi$  production data. We compare the  $K^-/\pi^-$  and  $K^+/\pi^+$  cross-section ratio data with calculations based on two global-fit parametrizations and two recent theoretical predictions for the kaon and pion PDFs, and test the results with two quarkonium production models. The  $K^-/\pi^-$  cross-section ratio for  $J/\psi$  production provides independent evidence of different valence quark distributions in pion and kaon. The  $K^+/\pi^+$   $J/\psi$  data are found to be sensitive to the gluon distribution in kaon. We show that these  $J/\psi$  production data provide valuable constraints for evaluating the adequacy of currently available sets of kaon PDFs.

The discovery of the partonic structures of nucleons in deep inelastic scattering (DIS) has led to extensive theoretical and experimental advances in our knowledge of the parton distribution functions (PDFs) in the proton. While the internal structures of the lightest mesons, the pion and the kaon, are of intense theoretical interest due to their dual roles as Goldstone bosons and quark-antiquark bound states, the corresponding experimental information is scarce. Recently, significant theoretical efforts have been devoted to the calculations of the quark and gluon distributions of the lightest mesons based on Lattice QCD [1, 2, 3] and various theoretical approaches [4, 5, 6, 7, 8, 9]. The partonic structures of mesons are also important for understanding the mass decomposition of hadrons [10, 11].

The early pion-induced Drell-Yan data from CERN and Fermilab [12, 13, 14] form the basis for extracting the valence quark distribution of the pion [15, 16, 17, 18, 19], while the sea-quark and gluon distributions are poorly determined from these data. Recently, the importance of pion-induced  $J/\psi$  data for constraining the quark and gluon distributions of pion was suggested [20, 21, 22, 23], leading to a new extraction of the pion PDFs from a global fit of pion-induced Drell-Yan and  $J/\psi$  production data in the statistical model approach [24].

The kaon PDFs are practically unknown experimentally, since the  $K^-$ -induced Drell-Yan data have only been measured by the NA3 collaboration with a limited statis-

tical accuracy [25]. Nevertheless, these data provide the evidence that the valence  $\bar{u}$  quark distribution of  $K^-$  is softer than that of  $\pi^-$ . This difference between the pion and kaon valence quark distributions is attributed to the breaking of the flavor SU(3) symmetry, resulting in a larger fraction of kaon's momentum being carried by the  $s$  quark than by the lighter  $\bar{u}$  quark. Further experimental inputs to access the valence quark as well as the gluon distribution of the kaon, are of much interest.

In this Letter, we investigate how the existing kaon-induced  $J/\psi$  production data can constrain kaon's valence quark and gluon distributions. In particular, the  $K^-/\pi^-$  cross-section ratio data for  $J/\psi$  production provide independent experimental evidence of a softer  $\bar{u}$  quark distribution of  $K^-$  than that of  $\pi^-$ . We also show that the  $K^+/\pi^+$  ratio is sensitive to the gluon distribution of the kaon.

The only available kaon-induced Drell-Yan data relevant for constraining the kaon PDFs were collected by the NA3 collaboration [25]. The  $K^-/\pi^-$  cross-section ratios were obtained from simultaneous measurements of the  $K^- + \text{Pt} \rightarrow \mu^+ \mu^- + \text{X}$  and  $\pi^- + \text{Pt} \rightarrow \mu^+ \mu^- + \text{X}$  reactions at 150 GeV. Figure 1 shows the Drell-Yan  $K^-/\pi^-$  ratio as a function of  $x_1$ , the fraction of the beam momentum carried by the interacting parton, for the dimuon events with mass  $M$  satisfying  $4.1 \leq M \leq 8.5$  GeV. The fall-off of the ratio at large  $x_1$  was interpreted by NA3 as evidence that the  $\bar{u}$  distribution in kaon is softer than that in pion [25].

In comparison with the Drell-Yan process, the significantly larger  $J/\psi$  production cross sections allow for measurements with much higher event rates. The NA3 col-

---

<sup>1</sup>changwc@phys.sinica.edu.tw

<sup>2</sup>jcpeng@illinois.edu

<sup>3</sup>Stephane.Platchkov@cern.ch

<sup>4</sup>sawada@icrr.u-tokyo.ac.jp

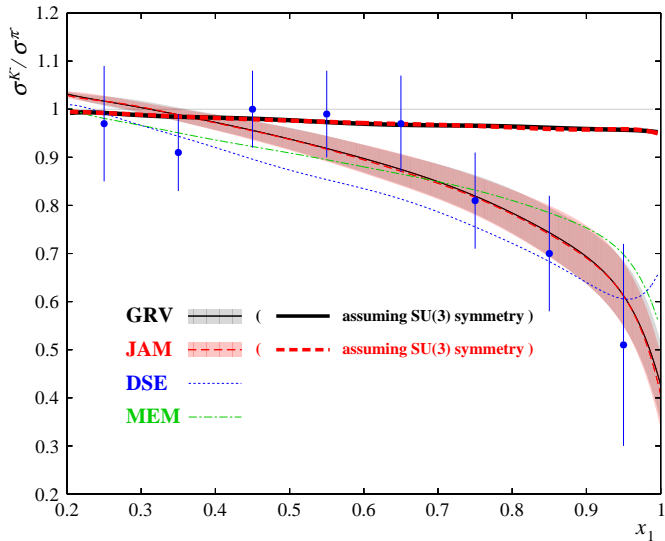


Figure 1: Ratios for  $K^-$  and  $\pi^-$ -induced Drell-Yan cross section as a function of the momentum fraction  $x_1$  on a platinum target with 150 GeV beams [25]. The solid black, dashed red, dotted blue and dot-dashed green curves are NLO Drell-Yan calculations using the GRV, JAM, DSE and MEM meson PDFs, respectively. The kaon PDFs for GRV and JAM are constructed using the expressions in Eqs.(1) and (2). The overlapping black and red bands denote the uncertainty range of  $\kappa$ . In addition, two thickened curves are the calculations using the GRV (solid black curve) and JAM (dashed red curve) meson PDFs assuming SU(3)-symmetric distributions for the pion and kaon.

laboration reported a measurement of  $K^-/\pi^-$  ratios on a platinum target at 150 GeV [26] (Fig. 2(a)). The data covered a broad range in  $x_F$  ( $x$ -Feynman) with good statistical accuracy. A comparison between Fig. 2(a) and Fig. 1 shows a striking similarity – while the  $K^-/\pi^-$  ratio approaches unity in the region of  $x_F < 0.6$ , it drops significantly as  $x_F$  increases. This similarity suggests a common origin for the pronounced drop at large  $x_1$  ( $x_F$ ) for the Drell-Yan ( $J/\psi$ )  $K^-/\pi^-$  cross-section ratios.

The NA3 collaboration also measured the  $K^+/\pi^+$  ratios for  $J/\psi$  production on a platinum target at 200 GeV [26] (Fig. 2(b)). Some differences between the  $K^+/\pi^+$  and the  $K^-/\pi^-$  ratios are noted when comparing Fig. 2(b) with Fig. 2(a) – while there is a pronounced drop at forward  $x_F$  for the  $K^-/\pi^-$  ratio, no such drop is observed for the  $K^+/\pi^+$  ratio. Moreover, the  $K^+/\pi^+$  ratios over the region  $0.0 < x_F < 0.7$  are  $\sim 20\%$  lower than the  $K^-/\pi^-$  ratios. As discussed below, these differences suggest that the  $K^+/\pi^+$  and  $K^-/\pi^-$  ratios are sensitive to different aspects of the kaon PDFs.

The only other measurement for kaon-induced  $J/\psi$  production was performed by the WA39 collaboration using a 39.5 GeV beam on a tungsten target [27]. Both the  $K^-/\pi^-$  and the  $K^+/\pi^+$   $J/\psi$  ratios were measured, as shown in Fig. 2(c) and Fig. 2(d), respectively. The  $K^+/\pi^+$  ratios at 39.5 GeV lie significantly lower than those at 200 GeV. As discussed later, the striking energy dependence of the  $K^+/\pi^+$   $J/\psi$  ratios reflects the difference in the domi-

nant process for  $J/\psi$  production at these two beam energies.

In order to calculate the  $K/\pi$  cross-section ratios consistently, we select theoretical approaches that provide both pion and kaon PDFs. The earliest attempt was made by Glück, Reya and Stratmann (GRS) [18], who obtained the pion PDFs using the constituent quark model. To account for the drop of the  $K^-/\pi^-$  Drell-Yan ratios at large  $x_1$ , GRS [18] proposed the following relations between the kaon and the pion valence-quark distributions:

$$\bar{u}_v^K(x) = N_u \bar{u}_v^\pi(x)(1-x)^\kappa, \quad (1)$$

where  $\bar{u}_v^K(x)$  and  $\bar{u}_v^\pi(x)$  correspond to the valence  $\bar{u}$  distributions in  $K^-$  and  $\pi^-$ , respectively. The value of  $\kappa$  was found to be 0.17 at the initial scale of  $0.34 \text{ GeV}^2$  for NLO calculations. The valence strange-quark distribution in  $K^-$  is assumed to be harder than  $\bar{u}_v^\pi(x)$ :

$$s_v^K(x) = 2\bar{u}_v^\pi(x) - \bar{u}_v^K(x). \quad (2)$$

The normalization factor  $N_u$  in Eq. (1), together with the expression of Eq. (2), ensures that the following sum rules for valence-quark distributions in kaon are satisfied:

$$\int_0^1 \bar{u}_v^K(x) dx = 1; \quad \int_0^1 s_v^K(x) dx = 1. \quad (3)$$

The GRS approach also assumes that the sea-quark and gluon distributions of the kaon are identical to those of the pion. The GRS ansatz of deriving the kaon's valence quark distributions is applied to the GRV [17] and JAM [28] global-fit pion PDFs to construct the individual corresponding kaon PDFs for the study. Another approach is the Continuum Schwinger function Methods [6], which is a covariant non-perturbative QCD approach for solving the Dyson-Schwinger Equations (DSE). The final one is the Maximum Entropy Method (MEM) [9] whose parameters for kaon PDFs were also obtained from a fit to the NA3  $K^-/\pi^-$  Drell-Yan data.

To begin, we first compare the NA3  $K^-/\pi^-$  Drell-Yan data with calculations using four different sets of meson PDFs, namely, GRV, JAM, DSE, and MEM. The calculations of the next-to-leading-order (NLO) Drell-Yan cross sections are performed using the DYNLO package [29]. The nuclear PDFs, EPPS16 [30], were used for the platinum target, although nuclear effects are expected to largely cancel in the cross-section ratios.

To illustrate the impact of the NA3 data on the kaon PDFs, we first present the calculations with GRV and JAM PDFs, by assuming that the kaon and pion PDFs are related by SU(3) symmetry. As shown by the two thickened solid black (GRV) and dotted red curves (JAM) in Fig. 1, both calculations fail to describe the data in the region of  $x_1 > 0.7$ .

The GRS ansatz is used for constructing the GRV and JAM kaon PDFs. The best-fit value of  $\kappa$  used to modify the valence quark distribution in Eq.(1), along with its  $1\sigma$  uncertainty, at the scale of Drell-Yan data is determined

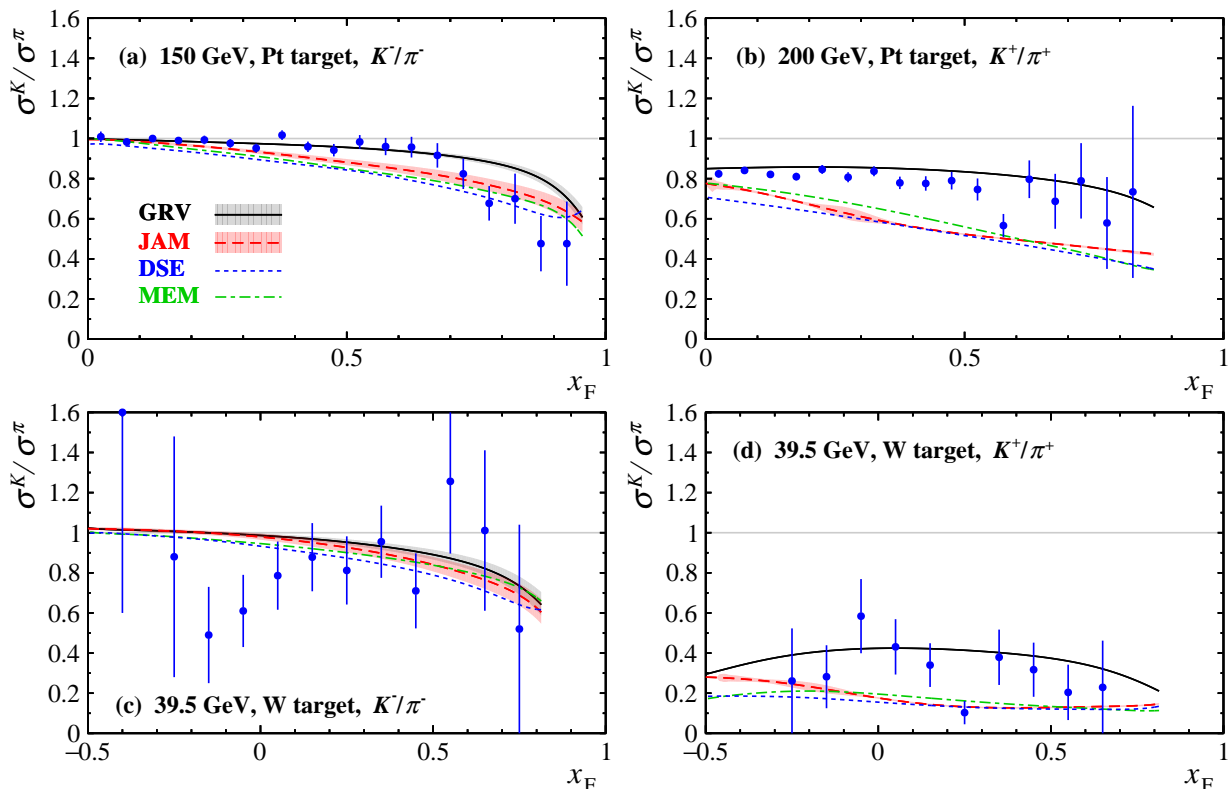


Figure 2: Cross-section ratios for  $J/\psi$  production versus  $x_F$ : (a)  $K^-/\pi^-$  at 150 GeV on a platinum target [26], (b)  $K^+/\pi^+$  at 200 GeV on a platinum target [26], (c)  $K^-/\pi^-$  at 39.5 GeV on a tungsten target [27], and (d)  $K^+/\pi^+$  at 39.5 GeV on a tungsten target [27]. The data are compared with NLO CEM calculations using various meson PDFs, denoted by the solid black, dashed red, dotted blue and dot-dashed green curves for the GRV, JAM, DSE and MEM meson PDFs, respectively. The black band denotes the uncertainty range of  $\kappa$  for GRV PDFs while the red one is the combined uncertainty of  $\kappa$  and the PDF uncertainty for JAM PDFs.

to be  $0.19 \pm 0.04$  by a NLO fit to the NA3  $K^-/\pi^-$  Drell-Yan data. The uncertainty range of  $\kappa$  is denoted by the black and red bands of modified GRV and JAM PDFs in Fig. 1. Because an SU(3) flavor symmetric sea is assumed in these pion PDFs from the global fits, the sea of the constructed kaon PDFs remains SU(3) flavor symmetric. After applying the GRS ansatz for the kaon PDFs, the GRV and JAM PDFs could describe the data nicely, like the DSE and MEM PDFs.

Since the kaon-induced  $J/\psi$  data were not included in the extraction of the above sets of kaon PDFs, it is of great interest to check how well these various sets of meson PDFs could describe the  $K/\pi$   $J/\psi$  production data. Such a comparison should provide additional insight and could help differentiate between these PDF sets. Unlike the Drell-Yan process, whose production mechanism is well understood, the precise mechanism for the  $J/\psi$  production remains a topic of active research. We take two theoretical approaches which are capable of reproducing many important features of the quarkonium production in hadron collisions. The first is the color evaporation model (CEM) at the next-to-leading order [31, 32], and the second is the nonrelativistic QCD (NRQCD) formalism [33, 34].

Both NLO CEM and NRQCD assume a factorization

of the quarkonium production into hard and soft parts. Perturbative QCD (pQCD) is used to calculate the short-distance hard part for the production of the  $c\bar{c}$  pairs in various color and spin states via  $GG$ ,  $q\bar{q}$  and  $qG$  subprocesses [35, 36]. Motivated by the quark-hadron duality, the CEM assumes a constant probability,  $F$ , for all different  $c\bar{c}$  states with an invariant mass  $M_{c\bar{c}}$  less than the  $D\bar{D}$  threshold, to hadronize into a given charmonium state. This assumption of a common factor for the hadronization of different subprocesses greatly reduces the number of parameters in the CEM. We also assume the same  $F$  for pion- and kaon-induced  $J/\psi$  production. For the production of the charm-quark pair, we utilize the NLO calculations described in Refs. [35, 36], widely used in the calculation of heavy-quark production. The final cross sections are obtained by a convolution of the hard and soft parts with the parton-parton luminosity of the associated meson and nucleon PDFs [21].

Figure 2 compares the  $J/\psi$  ratio data with the calculations using the four sets of meson PDFs. We find that the data are in excellent agreement with calculation based on the GRV PDFs, proposed more than two decades ago. The three more recent meson PDFs give very similar results, but do not agree with the data well. In particular,

they all predict much smaller values of the  $K^+/\pi^+$  ratios at 200 and 39.5 GeV. Moreover, they predict faster fall-off with  $x_F$  than the data for the  $K^-/\pi^-$  ratios at 150 GeV and  $K^+/\pi^+$  ratios at 200 GeV. Compared to the Drell-Yan  $K^-/\pi^-$  ratios data, the  $1\sigma$  uncertainty band in the  $K^-/\pi^-$  ratios is slightly reduced due to the dilution from the  $GG$  contribution. In the  $K^+/\pi^+$  ratios, the uncertainty band is significantly reduced due to the absence of valence-valence  $q\bar{q}$  contribution to the  $K^+$ -induced production. Although not shown in Fig. 1 and Fig. 2, we have also performed calculations using the SMRS meson PDFs [19] with results comparable to those obtained with GRV. Similarly, calculations using the xFitter meson PDFs [37] are very close to those of the JAM PDFs.

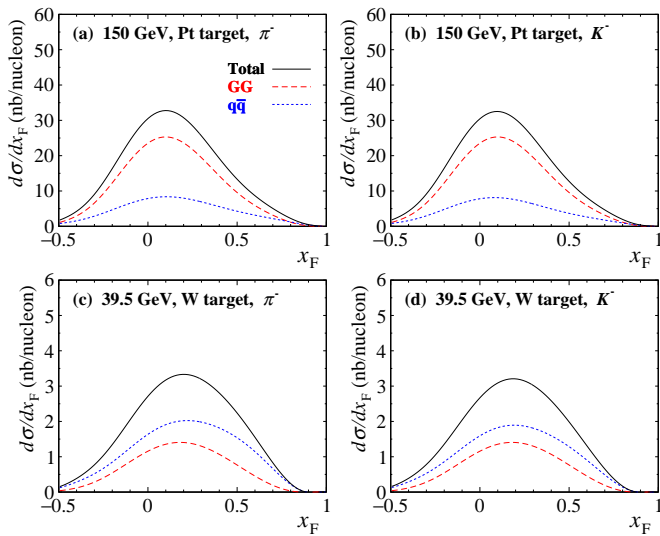


Figure 3: Cross sections for  $\pi^-$  and  $K^-$ -induced  $J/\psi$  production calculated using the NLO CEM with the GRV meson PDFs. The upper two plots, (a) and (b), are for a beam momentum of 150 GeV on a platinum target, and the lower two, (c) and (d), are for a beam momentum of 39.5 GeV on a tungsten target. The solid black curves are for the total production cross sections, and the dashed red and dotted blue curves are the contributions from the  $q\bar{q}$  annihilation and  $GG$  fusion subprocesses, respectively.

Since the most significant differences between the data and the calculations in Fig. 2 occur for the  $K^+/\pi^+$  ratios of  $J/\psi$  production, it is useful to explore the origin for these differences. In Figs. 3 and 4, the calculations of differential cross sections as a function of  $x_F$  for  $J/\psi$  production and the individual contributions of the  $q\bar{q}$  and  $GG$  channels are shown for the  $\pi^-$ ,  $K^-$ ,  $\pi^+$ , and  $K^+$  beams, respectively. These results are obtained using the NLO CEM calculation with the GRV meson PDFs, with the normalization factor  $F$  set to 0.05 [21]. Both  $\pi^-$  and  $K^-$  possess  $\bar{u}$  valence quarks so that the  $q\bar{q}$  contributions to the  $J/\psi$  production cross section are very similar. The  $GG$  fusion contributions are the same in both reactions. Therefore, the  $K^-/\pi^-$  ratios are close to 1 except decreasing slightly toward  $x_F = 1$  due to a softer  $\bar{u}(x)$  distribution in the kaon. In contrast, the  $K^+$  beam contains  $u$  and  $\bar{s}$  valence

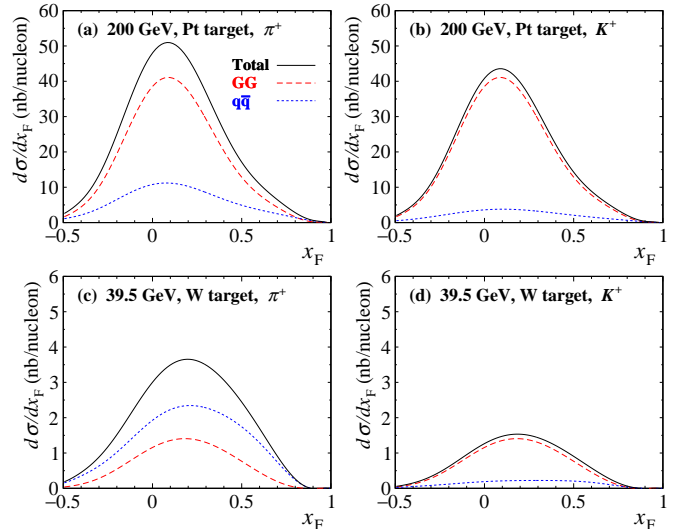


Figure 4: Same as Fig. 3, but for  $\pi^+$  and  $K^+$ -induced  $J/\psi$  production.

quarks, which can only annihilate with the sea quarks in the nucleons, while the  $\bar{d}$  valence quark in  $\pi^+$  can annihilate with the  $d$  valence quark in the nucleons resulting in additional contribution from the  $q\bar{q}$  annihilation. Consequently, the  $q\bar{q}$  contribution is suppressed compared to the  $GG$  fusion for the  $K^+$  beam and the  $K^+/\pi^+$  ratios turn out to be less than 1 and become very sensitive to the gluon distribution in the kaon. The prediction of a  $K^+/\pi^+$  ratio much lower than the data, as shown in Fig. 2 for the JAM, DSE, and MEM PDFs, is attributed to their kaon gluon distributions being smaller than required by the data.

Figure 5 shows the gluon ( $xG$ ) and valence  $u$  quark ( $xu_v$ ) distributions of the four kaon PDFs at the scale  $Q^2 = 9.6 \text{ GeV}^2$  relevant for  $J/\psi$  production. These distributions exhibit notable differences across the various PDFs. The rapid fall-off at large  $x$  for the JAM, DSE, and MEM gluon distributions in kaon is in contrast with the much slower drop of the GRV PDF. A behavior similar to that of the GRV is also observed for the SMRS PDF, not shown in Fig. 5.

We note that the pion and kaon gluon PDFs are set to zero at the initial scale for the DSE [6] and MEM [9] approaches, i.e., the gluon distribution at large  $Q^2$  is solely generated by the QCD parton radiation process. The gluon radiation from the heavier  $s$  quark in kaon is further suppressed with respect to that from the  $u$  and  $d$  quarks. In contrast, there is already a significant valence-like gluon distribution at the initial scale for the GRV meson PDFs [17].

The  $K^+/\pi^+$  ratio data for  $J/\psi$  production clearly favor a harder gluon distribution in pion and kaon than the parametrizations for the JAM, DSE, and MEM PDFs. This finding is consistent with observations made in a previous study [21] that the pion-induced  $J/\psi$  production data favor a gluon distribution in the pion that is harder

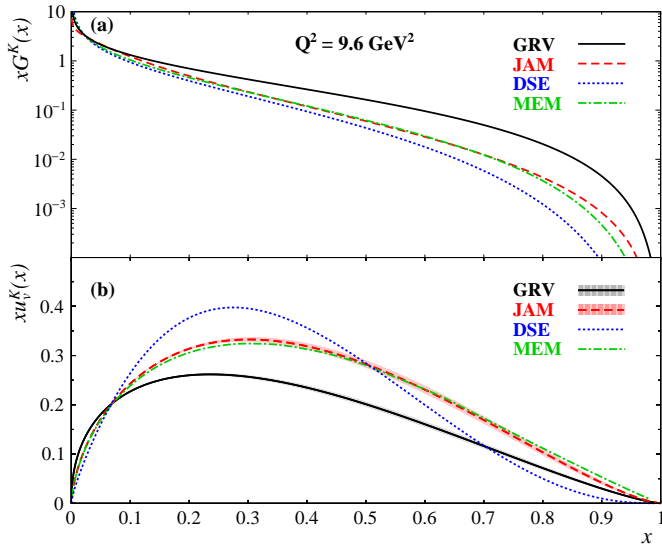


Figure 5: Distributions of the gluon ( $xG$ , (a)) and the valence  $u$  quark ( $xu_v$ , (b)) for the GRV, JAM, DSE, and MEM kaon PDFs. The black and red bands denote the uncertainty range of  $\kappa$  for GRV and JAM PDFs, respectively.

than the distributions in JAM and xFitter.

In order to check whether the evaluation of  $K/\pi$  ratios depends on the model used for the calculation of quarkonium production, we have also performed calculations using the NRQCD approach [34]. In NRQCD, the probability of a  $c\bar{c}$  pair hadronizing into a quarkonium bound state  $H$  ( $H = J/\psi$ ,  $\psi(2S)$ , or  $\chi_{cJ}$ ) is described by the long-distance matrix elements (LDMEs),  $\langle \mathcal{O}_n^H [^{2S+1}L_J] \rangle$ , depending on the spin, orbital, and total angular momentum quantum numbers,  $S$ ,  $L$  and  $J$ , respectively, and on the color configuration ( $n$ ) [22, 23, 34]. These LDMEs are assumed to be universal and independent of the beam species. Since the proton PDFs are well determined, the proton-induced data help in constraining the values of LDMEs common to all charmonium production data. A satisfactory description of  $J/\psi$  and  $\psi'$  production induced by pion and proton beams at fixed-target energies was recently achieved [23]. The extracted LDMEs [23] are used in the present analysis.

Figure 6 compares the  $K/\pi$  cross-section ratio data for  $J/\psi$  production with the calculations performed within the NRQCD framework using the four meson PDF sets. A comparison of Fig. 6 and Fig. 2 shows that qualitatively similar results are obtained for both theoretical approaches. The GRV kaon PDFs consistently give a better description of the data than the other three kaon PDFs. The finding that the data favor a harder gluon distribution in the kaon is also supported by the NRQCD calculations. The systematic variation of the scale and mass parameters in our CEM and NRQCD calculations of  $J/\psi$  production cross sections with pions has been extensively studied in Refs. [21, 22, 23]. The preference of the data for a harder pion gluon distribution remains unchanged for all these variations. In the current study of  $K/\pi$  ratios, systematic

uncertainties from the scale and mass parameters are expected to be greatly reduced due to cancellation. Other than the uncertainties of  $\kappa$  parameters, we also study the PDF uncertainties of JAM PDFs since its MC replicas are available. The variations of the  $K/\pi$  ratios due to the PDF uncertainties are found to be negligibly small, compared to those resulting from the uncertainties of the  $\kappa$  parameter. A similar study for the other PDFs like GRV, DSE, and MEM is not possible since the corresponding information on the PDF replicas is not available.

Although our analysis has focused on the  $K/\pi$  ratios for  $J/\psi$  production, we note that other experimental observables in kaon-induced  $J/\psi$  production are also of great interest. In particular, the difference between the  $K^-$  and  $K^+$ -induced  $J/\psi$  production cross sections on an isoscalar target, e.g.,  $\sigma_{J/\psi}(K^- + D) - \sigma_{J/\psi}(K^+ + D)$ , can provide a precise determination of the valence  $\bar{u}$ -quark distribution of the kaon. It can be readily shown that the above cross-section difference is proportional to the product of the valence  $\bar{u}$ -quark distribution of  $K^-$  and the valence quark distribution in the nucleon. A similar suggestion was considered earlier [38], but for the difference of Drell-Yan cross sections,  $\sigma_{DY}(K^- + D) - \sigma_{DY}(K^+ + D)$ . The much larger production cross sections for the  $J/\psi$  production than for the Drell-Yan process could provide an independent, high-statistics measurement of the valence  $\bar{u}$ -quark distribution of  $K^-$  in future kaon-induced  $J/\psi$  production experiments [39].

We summarize the main findings of this paper. First, we confirm that the ansatz proposed by the GRS [18], namely that the valence quark distributions for the kaon are related to that of the pion by Eqs. (1) and (2), and that the sea-quark and gluon distributions of the pion and kaon are identical, can satisfactorily describe the only existing  $K^-/\pi^-$  Drell-Yan ratio data from NA3. We then note that the  $K^-/\pi^-$   $J/\psi$  ratio data from NA3 provide independent evidence that the  $\bar{u}$  valence quark distribution of the kaon has a softer  $x$  distribution than that of the pion. The  $K^+/\pi^+$   $J/\psi$  ratio data are shown to be very sensitive to the gluon distribution of the kaon, and can be used to discriminate the various sets of existing kaon PDFs. In particular, the  $K^+/\pi^+$  ratio data for  $J/\psi$  production favor the GRV kaon PDFs, which have a gluon distribution larger than those obtained by JAM, DSE, and MEM. The good agreement obtained using the GRV PDFs would therefore indicate that the  $J/\psi$  ratio data are consistent with the scenario of nearly equal pion and kaon gluon distributions. These findings illustrate the usefulness of the  $J/\psi$   $K/\pi$  ratio data for constraining the poorly known kaon PDFs. A first attempt to extract the kaon PDF from these data using the statistical model was recently reported [40]. When new data on the kaon-induced Drell-Yan and  $J/\psi$  production anticipated at the AMBER experiment [39], together with the DIS data based on the Sullivan process proposed for the China EIC [41, 42] and U.S. EIC [43, 5], become available, further refinement in the parameterization of kaon PDFs could be considered.

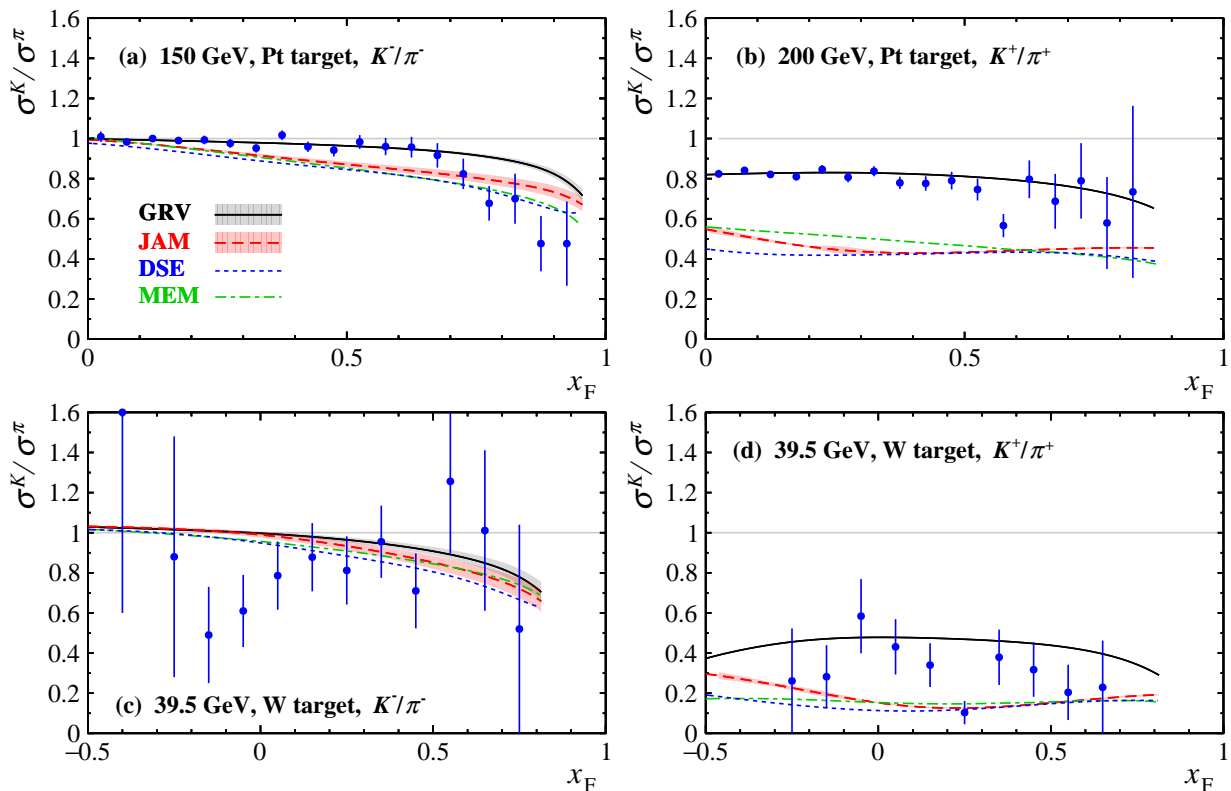


Figure 6: Same as Fig. 2, but for the NRQCD calculations.

For example, the requirements of the same valence quark momentum sum for kaon and pion, as well as the SU(3) flavor symmetry in the meson seas, could be relaxed in future global fits. Finally, persistent theoretical efforts to improve our understanding of the reaction mechanism involved in quarkonium production are of utmost importance for reducing the uncertainties in extracting the meson PDFs.

We acknowledge helpful discussions with Craig Roberts, Chengdong Han, Rong Wang, and Xurong Chen and information they provided on the DSE and MEM meson PDFs. This work was supported in part by the U.S. National Science Foundation Grant No. PHY-2210452 and the National Science and Technology Council of Taiwan (R.O.C.).

## References

- [1] H.-W. Lin, J.-W. Chen, Z. Fan, J.-H. Zhang, R. Zhang, Valence-Quark Distribution of the Kaon and Pion from Lattice QCD, *Phys. Rev. D* 103 (1) (2021) 014516. [arXiv:2003.14128](#), [doi:10.1103/PhysRevD.103.014516](#).
- [2] Z. Fan, H.-W. Lin, Gluon parton distribution of the pion from lattice QCD, *Phys. Lett. B* 823 (2021) 136778. [arXiv:2104.06372](#), [doi:10.1016/j.physletb.2021.136778](#).
- [3] A. Salas-Chavira, Z. Fan, H.-W. Lin, First glimpse into the kaon gluon parton distribution using lattice QCD, *Phys. Rev. D* 106 (9) (2022) 094510. [arXiv:2112.03124](#), [doi:10.1103/PhysRevD.106.094510](#).
- [4] T. Horn, C. D. Roberts, The pion: an enigma within the Standard Model, *J. Phys. G* 43 (7) (2016) 073001. [arXiv:1602.04016](#), [doi:10.1088/0954-3899/43/7/073001](#).
- [5] A. C. Aguilar, et al., Pion and Kaon Structure at the Electron-Ion Collider, *Eur. Phys. J. A* 55 (10) (2019) 190. [arXiv:1907.08218](#), [doi:10.1140/epja/i2019-12885-0](#).
- [6] Z.-F. Cui, M. Ding, F. Gao, K. Raya, D. Binosi, L. Chang, C. D. Roberts, J. Rodríguez-Quintero, S. M. Schmidt, Kaon and pion parton distributions, *Eur. Phys. J. C* 80 (11) (2020) 1064. [doi:10.1140/epjc/s10052-020-08578-4](#).
- [7] A. Watanabe, T. Sawada, C. W. Kao, Kaon quark distribution functions in the chiral constituent quark model, *Phys. Rev. D* 97 (7) (2018) 074015. [arXiv:1710.09529](#), [doi:10.1103/PhysRevD.97.074015](#).
- [8] J. Lan, C. Mondal, S. Jia, X. Zhao, J. P. Vary, Pion and kaon parton distribution functions from basis light front quantization and QCD evolution, *Phys. Rev. D* 101 (3) (2020) 034024. [arXiv:1907.01509](#), [doi:10.1103/PhysRevD.101.034024](#).
- [9] C. Han, G. Xie, R. Wang, X. Chen, An Analysis of Parton Distribution Functions of the Pion and the Kaon with the Maximum Entropy Input, *Eur. Phys. J. C* 81 (4) (2021) 302. [arXiv:2010.14284](#), [doi:10.1140/epjc/s10052-021-09087-8](#).
- [10] X.-D. Ji, Breakup of hadron masses and energy - momentum tensor of QCD, *Phys. Rev. D* 52 (1995) 271–281. [arXiv:hep-ph/9502213](#), [doi:10.1103/PhysRevD.52.271](#).
- [11] C. D. Roberts, D. G. Richards, T. Horn, L. Chang, Insights into the emergence of mass from studies of pion and kaon structure, *Prog. Part. Nucl. Phys.* 120 (2021) 103883. [arXiv:2102.01765](#), [doi:10.1016/j.pnpnp.2021.103883](#).
- [12] B. Betev, et al., Differential Cross-section of High Mass Muon Pairs Produced by a 194-GeV/ $c\pi^-$  Beam on a Tungsten Target, *Z. Phys. C* 28 (1985) 9. [doi:10.1007/BF01550243](#).
- [13] H. B. Greenlee, et al., The Production of Massive Muon Pairs in  $\pi^-$  Nucleus Collisions, *Phys. Rev. Lett.* 55 (1985) 1555. [doi:10.1103/PhysRevLett.55.1555](#).
- [14] J. S. Conway, et al., Experimental Study of Muon Pairs Produced by 252-GeV Pions on Tungsten, *Phys. Rev. D* 39 (1989) 92–122. [doi:10.1103/PhysRevD.39.92](#).

- [15] J. F. Owens,  $Q^2$ -dependent parametrizations of pion parton distribution functions, *Phys. Rev. D* 30 (1984) 943. doi:[10.1103/PhysRevD.30.943](https://doi.org/10.1103/PhysRevD.30.943).
- [16] P. Aurenche, R. Baier, M. Fontannaz, M. N. Kienzle-Focacci, M. Werlen, The gluon content of the pion from high- $p_T$  direct photon production, *Phys. Lett. B* 233 (1989) 517–521. doi:[10.1016/0370-2693\(89\)91351-8](https://doi.org/10.1016/0370-2693(89)91351-8).
- [17] M. Gluck, E. Reya, A. Vogt, Pionic parton distributions, *Z. Phys. C* 53 (1992) 651–656. doi:[10.1007/BF01559743](https://doi.org/10.1007/BF01559743).
- [18] M. Gluck, E. Reya, M. Stratmann, Mesonic parton densities derived from constituent quark model constraints, *Eur. Phys. J. C* 2 (1998) 159–163. arXiv:[hep-ph/9711369](https://arxiv.org/abs/hep-ph/9711369), doi:[10.1007/s100520050130](https://doi.org/10.1007/s100520050130).
- [19] P. J. Sutton, A. D. Martin, R. G. Roberts, W. J. Stirling, Parton distributions for the pion extracted from Drell-Yan and prompt photon experiments, *Phys. Rev. D* 45 (1992) 2349–2359. doi:[10.1103/PhysRevD.45.2349](https://doi.org/10.1103/PhysRevD.45.2349).
- [20] J.-C. Peng, W.-C. Chang, S. Platchkov, T. Sawada, Valence Quark and Gluon Distributions of Kaon from J/Psi Production arXiv:[1711.00839](https://arxiv.org/abs/1711.00839).
- [21] W.-C. Chang, J.-C. Peng, S. Platchkov, T. Sawada, Constraining gluon density of pions at large  $x$  by pion-induced  $J/\psi$  production, *Phys. Rev. D* 102 (5) (2020) 054024. arXiv:[2006.06947](https://arxiv.org/abs/2006.06947), doi:[10.1103/PhysRevD.102.054024](https://doi.org/10.1103/PhysRevD.102.054024).
- [22] C.-Y. Hsieh, Y.-S. Lian, W.-C. Chang, J.-C. Peng, S. Platchkov, T. Sawada, NRQCD analysis of charmonium production with pion and proton beams at fixed-target energies, *Chin. J. Phys.* 73 (2021) 13–23. arXiv:[2103.11660](https://arxiv.org/abs/2103.11660), doi:[10.1016/j.cjph.2021.06.001](https://doi.org/10.1016/j.cjph.2021.06.001).
- [23] W.-C. Chang, J.-C. Peng, S. Platchkov, T. Sawada, Fixed-target charmonium production and pion parton distributions, *Phys. Rev. D* 107 (5) (2023) 056008. arXiv:[2209.04072](https://arxiv.org/abs/2209.04072), doi:[10.1103/PhysRevD.107.056008](https://doi.org/10.1103/PhysRevD.107.056008).
- [24] C. Bourrely, W.-C. Chang, J.-C. Peng, Pion Partonic Distributions in the Statistical Model from Pion-induced Drell-Yan and  $J/\psi$  Production Data, *Phys. Rev. D* 105 (7) (2022) 076018. arXiv:[2202.12547](https://arxiv.org/abs/2202.12547), doi:[10.1103/PhysRevD.105.076018](https://doi.org/10.1103/PhysRevD.105.076018).
- [25] J. Badier, et al., Measurement of the  $K^-/\pi^-$  Structure Function Ratio Using the Drell-Yan Process, *Phys. Lett. B* 93 (1980) 354–356. doi:[10.1016/0370-2693\(80\)90530-4](https://doi.org/10.1016/0370-2693(80)90530-4).
- [26] J. Badier, et al., Experimental  $J/\psi$  Hadronic Production from 150 GeV/c to 280 GeV/c, *Z. Phys. C* 20 (1983) 101. doi:[10.1007/BF01573213](https://doi.org/10.1007/BF01573213).
- [27] M. J. Corden, et al., Experimental Results on  $J/\psi$  Production by  $\pi^\pm$ ,  $K^\pm$ ,  $p$  and  $\bar{p}$  Beams at 39.5-GeV, *Phys. Lett. B* 96 (1980) 411. doi:[10.1016/0370-2693\(80\)90799-6](https://doi.org/10.1016/0370-2693(80)90799-6).
- [28] P. C. Barry, N. Sato, W. Melnitchouk, C.-R. Ji, First Monte Carlo Global QCD Analysis of Pion Parton Distributions, *Phys. Rev. Lett.* 121 (15) (2018) 152001. arXiv:[1804.01965](https://arxiv.org/abs/1804.01965), doi:[10.1103/PhysRevLett.121.152001](https://doi.org/10.1103/PhysRevLett.121.152001).
- [29] S. Catani, L. Cieri, G. Ferrera, D. de Florian, M. Grazzini, Vector boson production at hadron colliders: a fully exclusive QCD calculation at NNLO, *Phys. Rev. Lett.* 103 (2009) 082001. arXiv:[0903.2120](https://arxiv.org/abs/0903.2120), doi:[10.1103/PhysRevLett.103.082001](https://doi.org/10.1103/PhysRevLett.103.082001).
- [30] K. J. Eskola, P. Paakkinen, H. Paukkunen, C. A. Salgado, EPPS16: Nuclear parton distributions with LHC data, *Eur. Phys. J. C* 77 (3) (2017) 163. arXiv:[1612.05741](https://arxiv.org/abs/1612.05741), doi:[10.1140/epjc/s10052-017-4725-9](https://doi.org/10.1140/epjc/s10052-017-4725-9).
- [31] R. Gavai, D. Kharzeev, H. Satz, G. A. Schuler, K. Sridhar, R. Vogt, Quarkonium production in hadronic collisions, *Int. J. Mod. Phys. A* 10 (1995) 3043–3070. arXiv:[hep-ph/9502270](https://arxiv.org/abs/hep-ph/9502270), doi:[10.1142/S0217751X95001443](https://doi.org/10.1142/S0217751X95001443).
- [32] R. E. Nelson, R. Vogt, A. D. Frawley, Narrowing the uncertainty on the total charm cross section and its effect on the  $J/\psi$  cross section, *Phys. Rev. C* 87 (1) (2013) 014908. arXiv:[1210.4610](https://arxiv.org/abs/1210.4610), doi:[10.1103/PhysRevC.87.014908](https://doi.org/10.1103/PhysRevC.87.014908).
- [33] G. T. Bodwin, E. Braaten, G. P. Lepage, Rigorous QCD analysis of inclusive annihilation and production of heavy quarkonium, *Phys. Rev. D* 51 (1995) 1125–1171, [Erratum: *Phys. Rev. D* 55, 5853 (1997)]. arXiv:[hep-ph/9407339](https://arxiv.org/abs/hep-ph/9407339), doi:[10.1103/PhysRevD.55.5853](https://doi.org/10.1103/PhysRevD.55.5853).
- [34] M. Beneke, I. Z. Rothstein, Hadroproduction of quarkonia in fixed target experiments, *Phys. Rev. D* 54 (1996) 2005, [Erratum: *Phys. Rev. D* 54, 7082 (1996)]. arXiv:[hep-ph/9603400](https://arxiv.org/abs/hep-ph/9603400), doi:[10.1103/PhysRevD.54.2005](https://doi.org/10.1103/PhysRevD.54.2005).
- [35] P. Nason, S. Dawson, R. K. Ellis, The total cross section for the production of heavy quarks in hadronic collisions, *Nucl. Phys. B* 303 (1988) 607–633. doi:[10.1016/0550-3213\(88\)90422-1](https://doi.org/10.1016/0550-3213(88)90422-1).
- [36] M. L. Mangano, P. Nason, G. Ridolfi, Fixed target hadroproduction of heavy quarks, *Nucl. Phys. B* 405 (1993) 507–535. doi:[10.1016/0550-3213\(93\)90557-6](https://doi.org/10.1016/0550-3213(93)90557-6).
- [37] I. Novikov, et al., Parton Distribution Functions of the Charged Pion Within The xFitter Framework, *Phys. Rev. D* 102 (1) (2020) 014040. arXiv:[2002.02902](https://arxiv.org/abs/2002.02902), doi:[10.1103/PhysRevD.102.014040](https://doi.org/10.1103/PhysRevD.102.014040).
- [38] J. T. Londergan, G. Q. Liu, A. W. Thomas, Kaon - nucleus Drell-Yan processes and kaon structure functions, *Phys. Lett. B* 380 (1996) 393–398. arXiv:[hep-ph/9604448](https://arxiv.org/abs/hep-ph/9604448), doi:[10.1016/0370-2693\(96\)00500-X](https://doi.org/10.1016/0370-2693(96)00500-X).
- [39] B. Adams, et al., Letter of Intent: A New QCD facility at the M2 beam line of the CERN SPS (COMPASS++/AMBER) arXiv:[1808.00848](https://arxiv.org/abs/1808.00848).
- [40] C. Bourrely, F. Buccella, W.-C. Chang, J.-C. Peng, Extraction of kaon partonic distribution functions from Drell-Yan and  $J/\psi$  production data, *Phys. Lett. B* 848 (2024) 138395. arXiv:[2305.18117](https://arxiv.org/abs/2305.18117), doi:[10.1016/j.physletb.2023.138395](https://doi.org/10.1016/j.physletb.2023.138395).
- [41] D. P. Anderle, et al., Electron-ion collider in China, *Front. Phys. (Beijing)* 16 (6) (2021) 64701. arXiv:[2102.09222](https://arxiv.org/abs/2102.09222), doi:[10.1007/s11467-021-1062-0](https://doi.org/10.1007/s11467-021-1062-0).
- [42] G. Xie, C. Han, R. Wang, X. Chen, Tackling the kaon structure function at EicC \*, *Chin. Phys. C* 46 (6) (2022) 064107. arXiv:[2109.08483](https://arxiv.org/abs/2109.08483), doi:[10.1088/1674-1137/ac5b0e](https://doi.org/10.1088/1674-1137/ac5b0e).
- [43] A. Accardi, et al., Electron Ion Collider: The Next QCD Frontier: Understanding the glue that binds us all, *Eur. Phys. J. A* 52 (9) (2016) 268. arXiv:[1212.1701](https://arxiv.org/abs/1212.1701), doi:[10.1140/epja/i2016-16268-9](https://doi.org/10.1140/epja/i2016-16268-9).